

REVIEW OF SELECTIVE ION SEPARATIONS AT BYU USING LIQUID MEMBRANE AND SOLID PHASE EXTRACTION PROCEDURES

REED M. IZATT

Department of Chemistry and Biochemistry

Brigham Young University

Provo, UT 84602, USA

Abstract. Research in selective ion separations at Brigham Young University has involved the use of liquid membranes of the bulk, emulsion, thin sheet supported, hollow fiber supported, and two-module hollow fiber supported types as well as solid phase extraction using immobilized ligands. By use of designed cation and anion selective macrocyclic ligands, it has been possible to accomplish a wide range of interesting separations. The principles underlying the separations and a comparison of the advantages and disadvantages of the various systems are given. Some of the solid phase extraction systems have been commercialized by IBC Advanced Technologies, Inc. Examples of commercial applications are presented in the analytical, environmental, metallurgical, precious metals, and nuclear waste areas.

Key words: Selective ion separations, macrocycle carriers, liquid membranes, solid phase extraction, analytical separations, environmental separations, metallurgical separations, precious metals separations, nuclear waste separations.

1. Introduction

The initiation of our effort to do chemical separations at Brigham Young University (BYU) in the late 1970s was preceded by extensive work on the synthesis of novel macrocycles [1,2] and on the thermodynamics of cation-ligand interactions [3-6]. Results by us and others [7-9] had shown that unique cation selectivities could be designed into host macrocycles. Early work on the thermodynamics of ion-macrocyclic interactions was summarized in a review [10]. Interest in macrocyclic chemistry received great impetus in the late 1960s when Pedersen [11,12] reported the preparation of cyclic polyethers and of their selective complexation properties for guest cations. The exciting possibility of being able to design pre-determined selectivity for specific guests into host molecules began, in the early 1970s, to attract workers from a variety of chemical fields. The significance of the diverse and voluminous studies that followed is reflected in the awarding of the 1987 Nobel Prize in Chemistry to Pedersen [13], Lehn [14], and Cram [15], three of the early investigators in the field.

Interest in macrocycles blossomed in separations science because of the promise these ligands showed for achieving effective, selective ion separations. Our early work in separations stemmed from a desire that my colleague, the late Professor J. J. Christensen, and I had to direct our research program toward practical applications. In 1977, we discussed our interest in using macrocycles in liquid membrane (LM) systems to accomplish selective metal ion separations with Dr. Walter Haubach at the Basic Energy Sciences Division of the Department of Energy. He expressed interest in our proposed work and the following year we began an effort on selective separations at BYU with Department of Energy support. This program has involved an appreciable number of faculty, post-doctoral associates, and graduate and undergraduate students. The results and insights gained in our work on facilitated cation transport in membrane systems led in 1987 to funding of solid phase extraction research (SPE) by the State of Utah Centers of Excellence program and, in 1988, to the establishment of IBC Advanced Technologies, Inc. (IBC) whose primary goal was and continues to be the development and marketing of commercial separations systems based on molecular recognition technology (MRT) concepts.

In the following sections, the use of LM and SPE systems to accomplish selective separations at BYU and IBC will be reviewed. Five LM systems used by us will be discussed with respect to the advantages and disadvantages of each, examples will be given to illustrate interesting characteristics of the systems and of carrier molecules, and comparisons will be made of separation data obtained using the various systems. Potential practical applications of the LM and SPE procedures will be discussed and examples will be given of SPE systems that have been commercialized by IBC. Further details on the cited results and references to earlier work by others are found in the literature references. Acknowledgment is given to my co-workers in each case as they are listed in the references cited.

2. Membrane Systems

2.1. GENERAL

The bulk (BLM), emulsion (ELM), thin sheet supported (TSSLM), hollow fiber supported (HFSLM), and two module hollow fiber supported (TMHFSLM) liquid membrane systems used in our work are depicted in Figure 1 [16,17]. Each operating system contains source, membrane, and receiving phases. The membrane phase in each case consists of an organic liquid and separates the source and receiving phases. In the supported systems, a matrix with pores accommodates the organic liquid. The organic liquid must have appropriately low solubility in both the source and receiving phases. The allowed solubility depends on the LM system used. The carrier molecule is present in the organic liquid. Achievement of optimum flux requires that the membrane solvent and carrier molecule be sufficiently insoluble in the source and receiving phases so that leakage to those phases is negligible. This requirement is particularly important in the cases of the TSSLM and HFSLM systems where volume ratios of aqueous to organic phases may reach 1000:1 or more. Kinetics was found to be diffusion controlled for all systems studied. The most reproducible data were obtained with the TSSLM system.

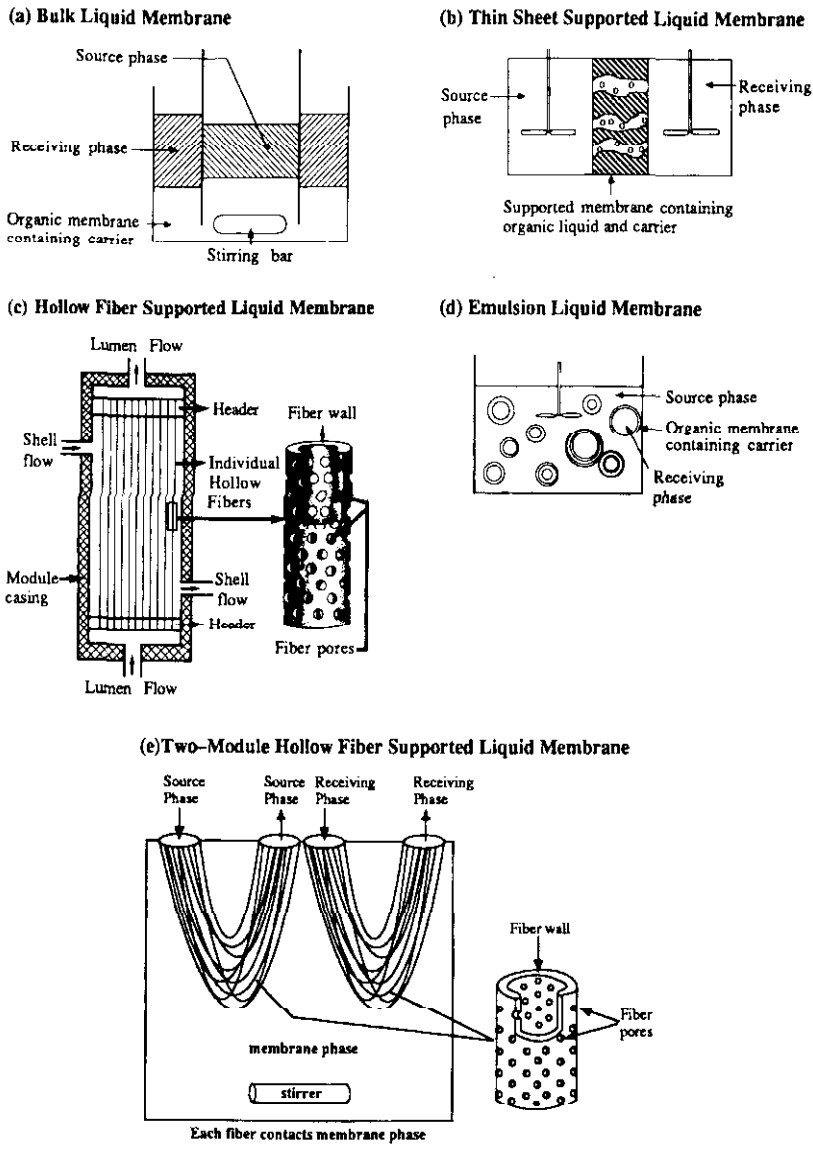


Figure 1. Liquid membrane types [17].

2.2. COMPARISON OF MEMBRANE SYSTEMS

The advantages and disadvantages of each of the membrane systems shown in Figure 1 for ion transport studies are summarized in Table I. The information in Table I is helpful in selecting a membrane system for a specific purpose.

Table I. Advantages and disadvantages of several liquid membrane systems [16-18].

Liquid Membrane System	Advantages	Disadvantages
Bulk (BLM)	<ol style="list-style-type: none"> 1. simple construction 2. small amounts of carrier used 3. useful for carrier screening 4. aqueous to membrane volume ratio small (~2:1) 	<ol style="list-style-type: none"> 1. small surface areas 2. slow transport rates 3. not commercially viable 4. difficult to reproduce experiments 5. large standard deviations in data 6. difficult to sort out surface active effects 7. variable geometry leads to difficulties in modeling
Emulsion (ELM)	<ol style="list-style-type: none"> 1. immense surface area 2. very rapid transport 3. large ratio of source to receiving phase volumes 4. large concentration of transporting species possible 5. potential for commercial use 	<ol style="list-style-type: none"> 1. moderately hydrophobic membrane solvent needed 2. moderately hydrophobic 3. macrocycle required 3. membrane stability can be adversely affected by pH, ionic strength, etc. and requires frequent monitoring 4. the emulsion must be broken to recover the receiving phase 5. variable geometry leads to difficulties in modeling

Thin sheet supported (TSSLM)	<ol style="list-style-type: none"> 1. small standard deviations in fluxes 2. measurable geometry leads to ease of modeling 3. results can predict hollow fiber membrane behavior under similar conditions 	<ol style="list-style-type: none"> 1. transport rates small 2. extremely hydrophobic membrane solvent and carrier required 3. system not commercially viable
Hollow fiber supported (HFSLM)	<ol style="list-style-type: none"> 1. rapid transport rates 2. easy introduction of source and receiving phases to system 	<ol style="list-style-type: none"> 1. surface active effects can lead to fouling 2. hydrophobic solvent necessary 3. extremely hydrophobic macrocycles needed 4. variable geometry leads to difficulty in modeling
Two module hollow fiber supported (TMHFSLM)	<ol style="list-style-type: none"> 1. easily accessible source, receiving, and membrane phases 2. rapid transport rates 3. continuous operation possible 4. does not require hydrophobic membrane solvents and carriers 5. has potential for industrial use 	<ol style="list-style-type: none"> 1. variable geometry leads to difficulty in modeling

The BLM system is useful for screening carriers. The small (milligram) concentrations of carriers required allow one to determine their transport ability even if only small amounts are available. On the other hand, transport rates are slow, experiments often have poor reproducibility, and the variable geometry of the system makes it difficult to model transport.

Very rapid transport rates can be obtained with the ELM system due to the large surface area present. This system also allows one to concentrate the transported species in the receiving phase. However, moderately hydrophobic membrane solvents and carriers are required. Difficulties generally associated with emulsion stability are present including effects of pH and ionic strength. Recovery of the species transported requires breaking the emulsion. Selectivity may be enhanced by addition of an appropriate complexing agent or by pH adjustment of the receiving phase.

The TSSLM system is advantageous because its geometry is known. In this system, there is good agreement between fluxes obtained from models and those derived from experimental data. A consequence of this is that the model may be used to identify and understand the relative importance of the factors involved in carrier-mediated ion transport processes. Use of the TSSLM system requires extremely hydrophobic membrane solvents in order to prevent drying out of the membrane. In addition, very hydrophobic carriers are required to prevent their loss to the aqueous phases during the experiment. In the TSSLM system used by us, the ratio of membrane to aqueous phases was approximately 1 to 1300 [17,19].

Rapid transport in a supported system is achievable by using a HFSLM system. TSSLM results may be used to predict HFSLM results under comparable experimental conditions. The HFSLM system may have commercial possibilities, but does suffer from potential membrane fouling problems and requires extremely hydrophobic membrane solvents and carriers.

Some of the disadvantages of the HFSLM system may be overcome by using the TMHFSLM system. In this case, much less hydrophobic solvents and carriers can be used. However, the variable geometry of the system makes modeling difficult.

2.3. REPRESENTATIVE SEPARATIONS IN MEMBRANE SYSTEMS

2.3.1. Bulk Liquid Membranes

Our early efforts involved the identification and investigation of parameters that influence the rates of macrocycle carrier-mediated transport of cations across liquid membranes. These parameters are discussed together with methods for optimizing their effect on transport and models of macrocycle-mediated transport in a review [20]. The effect of several of these parameters on transport are presented here.

For systems involving neutral macrocyclic carriers, an important factor is the nature of the anion that accompanies the cation-macrocycle complex across the membrane [21,22]. Indeed, for dibenzo-18-crown-6 (Figure 2) -mediated transport of K^+ across a

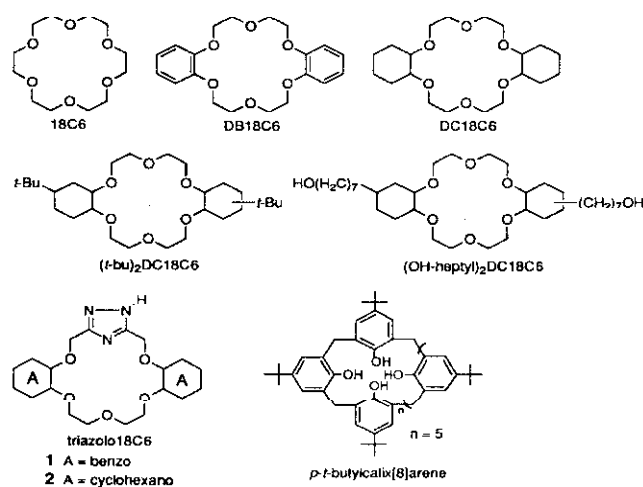


Figure 2. Macrocycles studied.

chloroform liquid membrane, the cation flux varied over eight orders of magnitude according to the anion present (Figure 3). An empirical linear correlation was found between the flux and the Gibbs free energy of hydration values for the anions.

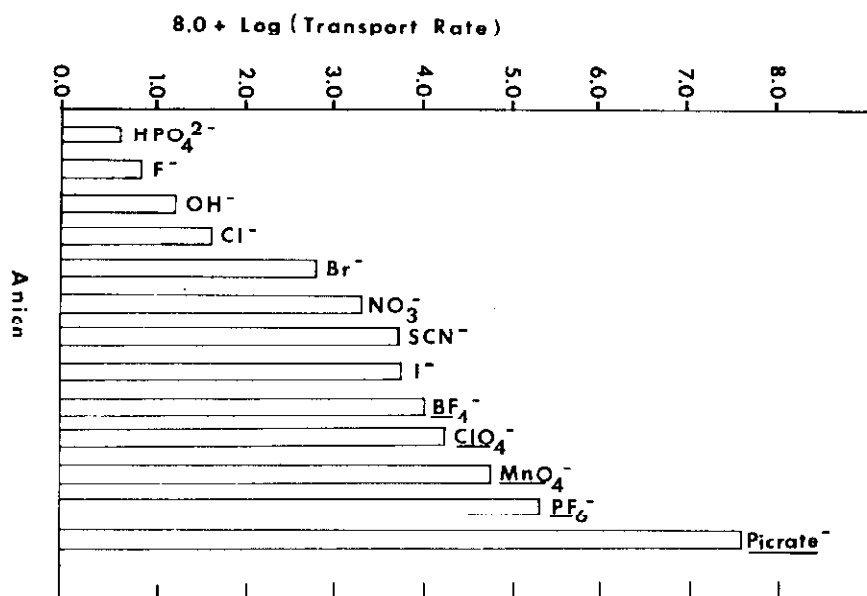


Figure 3. Variation of K⁺ transport rate across a CHCl₃ liquid membrane using DB18C6 as the carrier vs. the anion identity [22].

In 1975, Kirch and Lehn [23] demonstrated for a limited number of cases that a relationship exists between the equilibrium constants for cation-carrier interaction and the rates of individual cation transport through liquid membranes. Using a wide variety of macrocyclic carriers and metal ions, we showed that an optimum range in the log *K* values for cation-carrier interaction in methanol corresponded to maximum cation transport [24]. The rate of cation transport decreased rapidly at log *K* (CH₃OH) values higher or lower than this range. Log *K* (CH₃OH) values were used for these comparisons because CH₃OH was the only solvent with a low dielectric constant for which a wide variety of log *K* values were known. This effect is shown in Figure 4 [24] for the reaction of K⁺, Rb⁺, Sr²⁺, and Ba²⁺ with a variety of macrocycles. The solid curve results from a derived equation, which seems to predict the observed variation of cation transport rate with log *K* (CH₃OH) over a wide range of log *K* (CH₃OH) values.

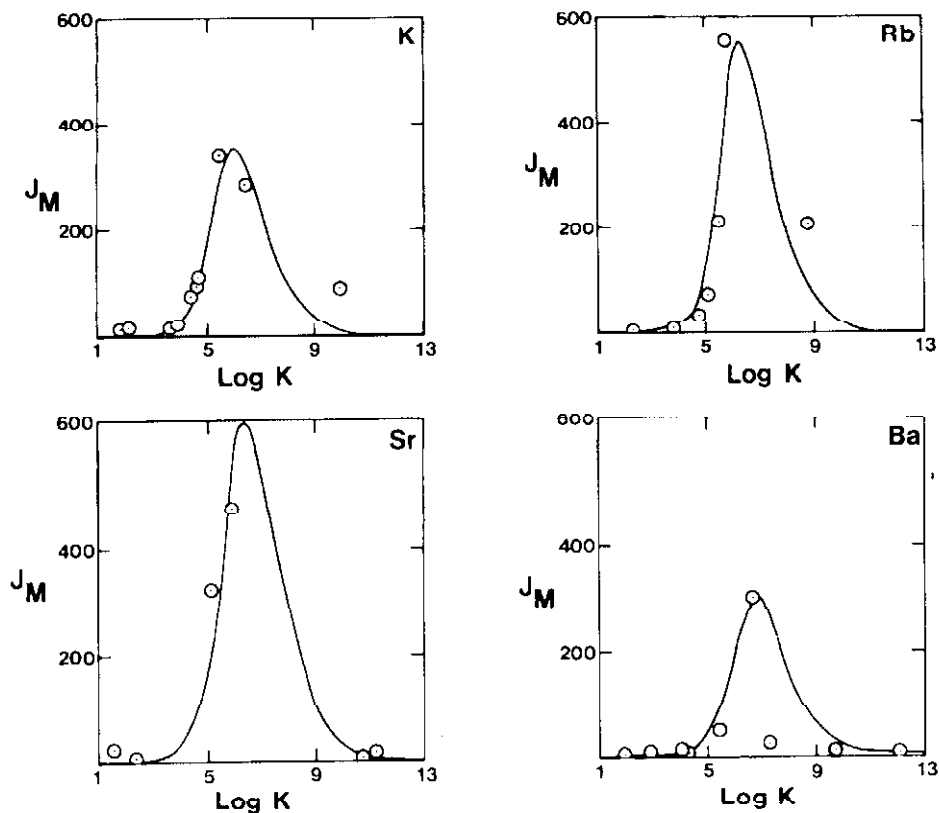


Figure 4. Plots of J_M vs. $\text{Log } K(\text{CH}_3\text{OH})$ for M^{n+} interaction with a variety of macrocycles [24]. The points represent experimental values and the solid line is derived from an equation.

The effect of other cations on the flux of a particular cation was of interest to us, since practical separations would involve such mixtures. The ability of DC18C6 (Figure 2) to transport Pb^{2+} selectively in binary mixtures of it and other cations was studied using the BLM system. High transport selectivities for Pb^{2+} were obtained even when the ratio of Pb^{2+} concentration to that of the other cation in the mixture was $<1/100$. The transport data are given in Table II. The higher competitive transport rate for Pb^{2+} in these mixtures is consistent with the higher $\text{log } K$ value for its interaction with DC18C6 [25].

Table II. Moles of Pb^{2+} and M^{n+} transported competitively from an aqueous source phase through a chloroform membrane containing the carrier DC18C6 to an aqueous receiving phase [25].

Source Phase ^a , $\text{Pb}^{2+}/\text{M}^{n+}$	DC18C6, ratio of moles transported ^b
$\text{Pb}^{2+}/\text{Li}^+$	300/0
$\text{Pb}^{2+}/\text{Na}^+$	240/1.0
$\text{Pb}^{2+}/\text{K}^+$	270/2.4
$\text{Pb}^{2+}/\text{Mg}^{2+}$	360/0.2
$\text{Pb}^{2+}/\text{Sr}^{2+}$	330/6.4
$(\text{Pb}^{2+}/\text{Ba}^{2+})^a$	260/2.9
$\text{Pb}^{2+}/\text{Fe}^{3+}$	340/0.07
$\text{Pb}^{2+}/\text{Cu}^{2+}$	250/0.02
$\text{Pb}^{2+}/\text{Zn}^{2+}$	320/0.06

^a Source phase is 0.5 M $\text{Pb}(\text{NO}_3)_2$ plus 0.5 M $\text{M}^{n+}(\text{NO}_3)_n$ in water, except where $\text{M}^{n+} = \text{Ba}^{2+}$, for which each salt was present at 0.15 M concentration.

^b Numbers are moles transported per 24 h reported as the average of three determinations; the reproducibility was $\pm 20\%$ or better.

The introduction of proton-ionizable macrocycles into the BLM system made it possible to couple metal ion transport with proton transport. An example of such a system is shown in Figure 5 where a calixarene is used as the carrier [26]. It is seen that transport of Cs^+ is negligible at pH values lower than about 11.5 but rises rapidly at higher pH values. The transport result is consistent with the idea that in the high pH region a proton

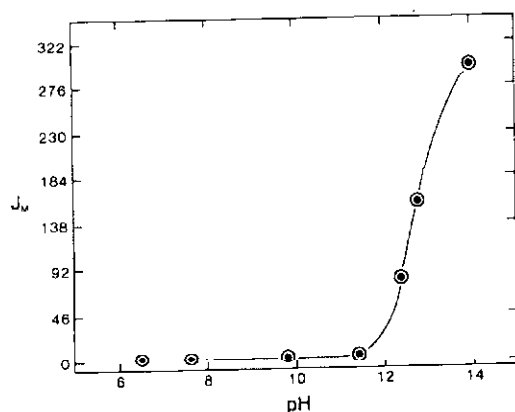


Figure 5. Plot of Cs^+ flux (J_M , mol $\times 10^8 / \text{s} \cdot \text{m}^2$) as a function of source phase pH in a BLM system [26]. Membrane: 0.001 M *p*-tert-butyl-calix[8]arene in 16% v/v $\text{CH}_2\text{Cl}_2/\text{CCl}_4$ solution. $[\text{Cs}^+] = 1 \text{ M}$. Anion = $\text{NO}_3^-/\text{OH}^-$. $T = 25^\circ \text{C}$.

is removed from the ligand and the resulting anion complexes with Cs^+ . It is apparent that for appreciable transport to occur, the aqueous source phase must be quite basic. At the receiving phase-membrane interface, Cs^+ is released and the calixarene anion extracts a proton from the H_2O or H_3O^+ present in the aqueous phase. Thus, Cs^+ transport is coupled with H^+ transport using this carrier. It is instructive to compare the effect of pH and anion on the single ion transport of Na^+ , K^+ , Rb^+ , and Cs^+ using 18C6 and calix[8]arene as the carrier molecules [27]. The results in Table III show that for 18C6, a neutral carrier, large

Table III. Cation transport of alkali metal ion nitrates and hydroxides through halocarbon liquid membranes^a using 18-crown-6 and *p*-*tert*-butylcalix[8]arene as carriers [26,27].

Source Phase	Flux ($\times 10^{-8} \text{ mol s}^{-1} \text{ m}^{-2}$)		Source Phase	Flux ($\times 10^8 \text{ mol s}^{-1} \text{ m}^{-2}$)	
	18C6	Calix [8] arene		18C6	Calix [8]arene
NaNO_3	25	<i>b</i>	NaOH	<i>c</i>	9
KNO_3	645	<i>b</i>	KOH	<i>c</i>	10
RbNO_3	484	<i>b</i>	RbOH	<i>c</i>	340
CsNO_3	161	<i>b</i>	CsOH	<i>c</i>	996

^aMembranes: 0.001 M *p*-*tert*-butylcalix[8]arene in 25% v/v $\text{CH}_2\text{Cl}_2/\text{CCl}_4$; 0.001 M 18C6 in CHCl_3 .

^b Less than $0.7 \times 10^{-8} \text{ mol/s}\cdot\text{m}^2$.

^c Less than $0.9 \times 10^{-8} \text{ mol/s}\cdot\text{m}^2$.

transport rates are achieved from solutions containing nitrate ion, but not from those containing OH^- . This result is consistent with the large solvation energy of OH^- compared to NO_3^- as mentioned earlier and illustrated in Figure 3. On the other hand, the proton-ionizable calix[8]arene shows no transport from solutions containing nitrate salts, but high transport from solutions with high OH^- concentrations. The data also show that K^+ is selectively transported by 18C6 and Cs^+ by the calix[8]arene. Selectivity for Cs^+ by the calix[8]arene and other calixarenes is maintained in competitive transport experiments from binary and ternary mixtures of the alkali metal ions [27]. Competitive transport of metal ions from multi-cation mixtures was studied using a variety of macrocyclic carriers [28-30].

Results for transport of equimolar $\text{Ag}(\text{NO}_3)$ and $\text{Pb}(\text{NO}_3)_2$ in a BLM using a proton-ionizable triazole carrier demonstrate how selectivity for Ag^+ over other univalent and bivalent cations can be designed into a transport system [31]. The data in Table IV show that in each single cation experiment transport of Ag^+ is much greater into an acidic than a neutral receiving phase. However, the receiving phase pH had little effect on the transport of Pb^{2+} . In the competitive systems, selective transport of Ag^+ over Pb^{2+} was enhanced in each case by an acidic receiving phase. These results suggest that in cases involving acid receiving phases Ag^+ is being transported by a proton-ionizable-carrier mechanism, while Pb^{2+} transport is by a neutral mechanism. If Pb^{2+} transport were by a

proton-ionizable mechanism, the addition of acid to the receiving phase should enhance that transport. The transport data in Table IV show that this is not the case.

Table IV. Comparison of single and competitive Ag^+ and Pb^{2+} fluxes^a in a BLM system^b containing triazole macrocycles^c and either neutral or acidic receiving phases [31].

Carrier	Initial receiving-phase pH	Single Systems		Competitive Systems $\text{Ag}^+/\text{Pb}^{2+}$ fluxes
		Ag^+ flux	Pb^{2+} flux	
1	7	61	2	47/<1
1	1.5	182	2.5	288/<1
2	7	269	322	720/7
2	1.5	1125	326	1549/8

^a Flux in units of $\text{mol} \cdot \text{s}^{-1} \cdot \text{m}^{-2} \times 10^8$. Mean values of at least three experiments with standard deviations less than $\pm 25\%$.

^b Source phase: 1 M AgNO_3 , 1 M $\text{Pb}(\text{NO}_3)_2$ or 0.5 M $\text{Ag}(\text{NO}_3)$, 0.5 M $\text{Pb}(\text{NO}_3)_2$. Membrane phase: 1×10^{-3} M carrier in CH_2Cl_2 . Receiving phase: H_2O or 0.031 M HNO_3 (pH 1.5).

^c Structures are given in Figure 2.

Further examination of the two possible transport mechanisms was made by determining the amount of NO_3^- transported. In the case of the water receiving phases, two nitrate ions were transported with each Pb^{2+} and one nitrate ion was transported with each Ag^+ . These results indicate that these metal ions were transported by a neutral carrier mechanism. A different result was obtained when the receiving phase was acidic. In the case of Ag^+ , the presence of a HNO_3 receiving phase resulted in significant changes in the source and receiving phase pH values during transport, indicating that protons were being transferred from the receiving to the source phase. Thus, in the presence of an acidic receiving phase, Ag^+ transport occurs by a proton-ionizable mechanism. In the case of Pb^{2+} with either phase and of Ag^+ with a H_2O receiving phase, only slight pH changes were observed, confirming that the neutral mechanism was dominant.

In the competitive systems in Table IV, the enhanced selectivity of Ag^+ over Pb^{2+} when a HNO_3 receiving phase is present is of interest. As in the analogous single cation case, Ag^+ transport is by a proton-ionizable mechanism while NO_3^- is co-transported with Pb^{2+} . The result is that Ag^+ is transported much more rapidly than Pb^{2+} . This result suggests that the incorporation of a proton-ionizable site can be used to design macrocycles to be highly selective carriers for Ag^+ over multivalent cations. Furthermore, the triazole carriers have a large complexation preference for Ag^+ over other univalent ions (alkali metal ions and Tl^+) resulting in minimal transport with these cations. Thus, Ag^+ can be transported selectively over all other cations using these carriers. These results were confirmed by ELM experiments [31].

2.3.2. Emulsion Liquid Membranes

The ELM system has a very thin membrane and an enormous membrane surface resulting in very rapid transport of solute from the source phase to the receiving phase. Concentration of the transported species by a large factor is accomplished by proper selection of source and receiving phase volumes. Movement of the solute to the receiving phase can be further facilitated by adding a species in the latter phase that has high affinity for the transported ion(s). A useful feature of ELM systems is that by altering certain of their properties a wide variety of selective separations is possible. These properties include the nature of the metal in the source phase, the macrocycle in the membrane phase, and the receiving phase anion. Adjustment of these properties led to a number of interesting separations using these membranes, several of which are now illustrated.

Relative transport rates of metal cation nitrates (Na^+ , K^+ , Rb^+ , Cs^+ , Ag^+ , Tl^+ , Ca^{2+} , Sr^{2+} , Ba^{2+} , and Pb^{2+}) in a water-toluene-water ELM were determined [32]. The toluene membrane contained the surfactant Span-80 (sorbitan monooleate, 3% v/v) and DC18C6. The aqueous receiving phase contained $\text{Li}_4\text{P}_2\text{O}_7$. Transport rates were determined both for individual cations and for equimolar binary cation mixtures of either Tl^+ or Pb^{2+} with M^{n+} . For individual transport, the order was $\text{Tl}^+ > \text{Ag}^+ > \text{Rb}^+ > \text{Cs}^+ > \text{K}^+ > \text{Na}^+$ and $\text{Pb}^{2+} > \text{Sr}^{2+} > \text{Ba}^{2+} > \text{Ca}^{2+}$. Some of the cations were concentrated nearly ten-fold in ten minutes. A marked change in the transport rates was found in the binary mixtures. Tl^+ , when present with either Na^+ , Cs^+ , or Rb^+ was selectively extracted from the source phase. Complete and nearly exclusive extraction of Pb^{2+} was observed in the presence of all cations studied including Tl^+ . The ability of Pb^{2+} to essentially stop transport of all other cations in the binary mixtures is attributed to two causes. First, the $\log K(\text{H}_2\text{O})$ value for Pb^{2+} -DC18C6 interaction is much larger than that for any of the other cations [33]. Thus, there is preferential interaction of Pb^{2+} with DC18C6 at the source phase-membrane phase interface. Second, the $\log K(\text{H}_2\text{O})$ value (10.1) for Pb^{2+} - $\text{P}_2\text{O}_7^{4-}$ interaction is much larger than that (<6) for any of the other cations [32]. Therefore, Pb^{2+} is transferred preferentially to the receiving phase. The presence of $\text{P}_2\text{O}_7^{4-}$ insures complete transport of Pb^{2+} to the receiving phase. Similar arguments can be made to account for the preferential transport of Tl^+ over the alkali metal ions in their binary mixtures.

The importance of the anion in the receiving phase in affecting transport selectivity is illustrated by DC18C6-mediated ELM experiments using a toluene membrane in which Pb^{2+} and Ag^+ are present in the source phase, but $\text{S}_2\text{O}_3^{2-}$ is present in the receiving phase [34]. In this case, Ag^+ is transported preferentially to Pb^{2+} . On the other hand, when $\text{P}_2\text{O}_7^{4-}$ is present in the receiving phase, Pb^{2+} is transported in preference to Ag^+ . These results are consistent with the observations that both metal ions form stable complexes with DC18C6 [33], $\log K(\text{H}_2\text{O})$ values for 1:1 complexation with $\text{S}_2\text{O}_3^{2-}$ are 8.87 for Ag^+ and 2.56 for Pb^{2+} , and analogous $\log K(\text{H}_2\text{O})$ values with $\text{P}_2\text{O}_7^{4-}$ are unknown for Ag^+ and 10.1 for Pb^{2+} [32]. The Ag^+ - $\text{P}_2\text{O}_7^{4-}$ $\log K(\text{H}_2\text{O})$ value is apparently small.

A requirement for effective transport is that the metal ion interact appreciably with the carrier at the source phase-membrane phase interface. This requirement is illustrated by results with Ca^{2+} and Mg^{2+} [34]. Neither of these cations forms stable complexes with DC18C6, but each forms a stable complex with $\text{P}_2\text{O}_7^{4-}$, Ca^{2+} ($\log K = 5.60$), Mg^{2+} ($\log K = 5.7$). Transport of these ions is negligible in the ELM system.

In two papers [35,36], we explored the role of the anion, SCN^- , on DC18C6-facilitated separations of univalent silver and bivalent cadmium, mercury, and zinc in ELM systems.

The separations were accomplished from various binary equimolar mixtures of the metals in the source phase. This phase also contained SCN^- in predetermined amounts. The separation results demonstrate that a neutral metal- SCN^- entity is necessary for the effective extraction of the metal-anion-DC18C6 complex into the membrane phase. This principle is illustrated by the selective transport of Cd(II) over Ag(I) [36]. In this case, the ELM system consisted of (1) an aqueous source phase containing $0.001\text{M Cd(NO}_3)_2$ and 0.001M AgNO_3 and varying concentrations of Mg(SCN)_2 , (2) a toluene membrane containing DC18C6 (0.02 M) and the surfactant SPAN 80, and (3) an aqueous receiving phase containing MgS_2O_3 or $\text{Mg(NO}_3)_2$. Mg^{2+} was used because it had negligible transport under the experimental conditions of the experiment. The disappearance of each metal was determined as a function of time.

The transport rate of Cd(II) was highest when a maximum amount of the Cd(II) in the source phase was present as $\text{Cd(SCN)}_2(\text{aq})$. This occurred at $[\text{SCN}^-] = 0.4\text{ M}$. Under these conditions, Cd(II) was transported over Ag(I) , which was present mainly as Ag(SCN)_4^{3-} by 5- and 55- fold in 5 minutes with 0.4 M SCN^- in the source phase and $0.3\text{ M S}_2\text{O}_3^{2-}$ and 0.3 M NO_3^- , respectively, in the receiving phase. The total percent of Cd(II) transported in the competitive experiments was 98 and 84, respectively. These results were explained using the various $\log K$ values for cation-DC18C6, cation- SCN^- and cation- $\text{S}_2\text{O}_3^{2-}$ interactions. The results indicate that rapid transport occurs when experimental conditions are adjusted so that the target cation is present in the source phase as a neutral complex and the other cations are in an ionic form. Figure 6 illustrates the neutral bivalent metal species that should have maximum transport. The Ag(SCN)_4^{3-} species would not be

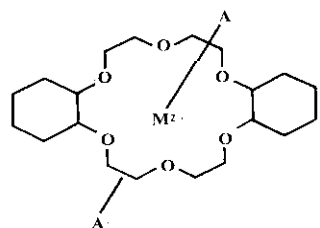


Figure 6. Schematic representation of an M^{2+} -DC18C6 (A^-)₂ complex [36].

expected to transport by this mechanism. The increased transport of Ag(I) when $\text{S}_2\text{O}_3^{2-}$ is present in the receiving phase indicates that a small amount of Ag(I) is present as $\text{Ag(SCN)}(\text{aq})$ and this moves to the receiving phase because of the large affinity of Ag^+ for $\text{S}_2\text{O}_3^{2-}$.

2.3.3. Thin Sheet Supported Liquid Membranes

The membranes discussed to this point allow one to study separations involving a variety of interesting host-guest systems. However, the geometry of these membranes cannot be determined making it impossible to model them accurately. The TSSLM system allows one to model transport and compare the results to those obtained experimentally.

The characterization of our TSSLM system has been reported [19]. As can be seen in the description in Fig. 1, the volume of the pores in the supported Celgard liquid membrane is much smaller than that of the combined source and receiving phases. It was estimated that the volume ratios were about 1:1333 [17]. In order for this membrane to

function properly, a solvent and a macrocycle are required that have extremely low solubilities in water. In addition, the macrocycle must be soluble in the solvent used. A number of solvents were tested including (water solubility in wt.% in parentheses) chloroform (0.71), toluene (0.063), 1,2-dichlorobenzene (0.0145), and phenylhexane (no data available). The ability of each of these solvents to form an impermeable barrier to KNO_3 movement from source to receiving phase was tested. In the case of chloroform, K^+ began to appear in the receiving phase almost immediately after the transport cell was assembled indicating loss of the solvent to the adjoining phases. In the cases of toluene and 1,2-dichlorobenzene, K^+ began to appear after several hours. For phenylhexane, no K^+ appeared in the receiving phase even after several days. Thus, phenylhexane was considered to be a suitable membrane solvent for the study, since each experiment would last about 24 h.

It was desirable to use a carrier molecule with a large membrane solvent/water distribution coefficient. This feature has the advantages that a negligible amount of the carrier is lost to the aqueous phase and all of the carrier is available for the transport process. Distribution coefficients for the macrocycles of interest were not available for phenylhexane. However, some values are available for toluene, which is similar in structure. Distribution coefficients for DC18C6 and di(*tert*-butylcyclohexano)-18-crown-6 between toluene and water are 13.3 and > 999 . It is apparent that the *t*-butyl groups cause a marked decrease in water solubility of the second compound. We reasoned that the introduction of two 1-hydroxyheptyl groups to DC18C6 should decrease the solubility even further. In addition, maintaining the DC18C6 structure should insure that the selective cation interactions observed with this ligand would be found with the more hydrophobic macrocycles. The validity of these assumptions is illustrated by the results in Table V [19]. The low flux by DC18C6 probably reflects the loss of this ligand to the adjoining aqueous phases as soon as the apparatus is assembled. On the other hand, the two remaining macrocycles have high flux values in the case of K^+ and show the expected high selectivity of the DC18C6 moiety for K^+ over Na^+ and Li^+ . The integrity of the membrane is maintained in these latter cases. Further work with (HO-heptyl)₂DC18C6

Table V. Macrocycle-mediated transport of Li^+ , Na^+ , and K^+ through a supported Celgard membrane^a [19].

Macrocycle carrier	Flux ($\text{mol}\cdot\text{sec}^{-1}\cdot\text{m}^{-2}$) $\times 10^8$		
	Li^+	Na^+	K^+
DC18C6	0	<0.01	<0.01
(<i>t</i> -bu) ₂ DC18C6 ^b	0	<0.1	3.6 ± 0.7
HO-heptyl ₂ DC18C6 ^c	0	<0.05	3.6 ± 0.2

^a Phase compositions: source phase 0.1M in each of LiNO_3 , NaNO_3 , and KNO_3 ; membrane phase, Celgard 2400 film saturated with phenylhexane 0.05M in the macrocycle carrier; receiving phase, water.

^b Di(*tert*-butylcyclohexano)-18-crown-6

^c Dihydroxyheptyl-dicyclohexano-18-crown-6

showed that the membrane was stable up to 24 hours, the duration of the experiments. The flux of the cations in this system was low signifying that the concentrations of the source and receiving phases changed little during the course of the experiments. Plots of concentration vs. time were linear in all cases. The cation transport was found to be diffusion-limited.

One of our goals was to model diffusion-limited, neutral macrocycle-mediated cation transport in the TSSLM system. This was accomplished using a variety of single cation and multiple cation systems [37]. The model parameters used were membrane geometry, solute diffusion coefficient in the membrane, initial phase constituent concentrations and speciation, and an equilibrium constant for the extraction process. The model was also revised to account for macrocycle loss from the membrane by including the partition coefficient of the macrocycle and equilibrium constants for aqueous cation-macrocycle interactions.

Comparison of single cation and competitive cation fluxes as predicted from the model and observed from experiment is given in Table VI. Details of the model and of the experimental results are available [37]. The results in Table VI show that there is good agreement between the predicted and experimental (observed) values for a variety of systems. All of the model parameters are either readily measured or calculated. These parameters allow one to distinguish the effects on transport fluxes and selectivities of cation, anion, and macrocycle type and concentration. Thus, the model has important usefulness in separating out and evaluating the various effects important in transport and selectivity. The separations and selectivities observed may be related to the molecular properties of the macrocycles involved. This, in turn, may be an aid in the design of macrocycles to perform desired separations, and in the rapid testing of such macrocycles.

2.3.4. *Hollow Fiber Supported Liquid Membrane*

The model for the TSSLM system was adjusted to cylindrical coordinates and tested for use in a HFSLM system [38]. The HFSLM system makes rapid transport possible while maintaining the selectivity of the TSSLM system. The data comparing predicted and observed fluxes are given in Table VII. Good agreement is seen. Compared to the ELM system, the HFSLM requires a much smaller inventory of solvent and carrier since the volume ratios of the two aqueous phases to the membrane are large. However, the large volume ratios are a disadvantage in that very hydrophobic membrane solvents and carriers are required to maintain membrane integrity and operate the system.

2.3.5. *Two Module Hollow Fiber Supported Liquid Membrane*

The TMHFSLM system was developed to overcome the necessity of using very hydrophobic membrane solvents and carriers [38]. As indicated in Table I, accomplishment of this goal gives this system significant advantages over the HFSLM system. In Figure 1e, the operating system is depicted. The ratio of the volumes of the aqueous and organic phases is about 17:1 making it possible to use membrane solvents and carrier reagents of low hydrophobicity. It is also seen that additional membrane solvent and carrier reagent are easily added to replace those lost during operation. This ease of replacement is a large advantage over either the ELM or HFSLM system [17].

Table VI. Predicted and observed single cation and competitive cation fluxes (J^*) [37].

Source Phase		$10^8 J$	
M^{n+}	A^-	Predicted	Observed
<u>Single Cation</u>			
Cd^{2+}	$Br^- (0.56M)$	83	89 ± 5
	$Br^- (0.20 M)$	74	79 ± 1
	$SCN^- (0.85 M)$	1100	1010 ± 10
	$SCN^- (0.10 M)$	670	650 ± 20
	$Cl^- (0.56 M)$	1.6	2.5 ± 0.3
Pb^{2+}	$NO_3^- (0.66 M)$	33.0	31 ± 4
K^+	$NO_3^- (0.2 M)$	13.0	12.0 ± 0.5
<u>Competitive Cation</u>			
1. K^+	$NO_3^- (0.1 M)$	5.3	3.6 ± 0.7
Na^+	$NO_3^- (0.1 M)$	<i>b</i>	0.06 ± 0.02
Li^+	$NO_3^- (0.1 M)$	<i>b</i>	<i>b</i>
2. Ba^{2+}		0.6	0.8 ± 0.1
Sr^{2+}		1.6	2.1 ± 0.1
Ca^{2+}		<i>b</i>	<i>b</i>
3. $Cd(II)$		81.0	71 ± 2
$Zn(II)$		<i>b</i>	<i>b</i>

^a Units of $mol \cdot s^{-1} \cdot m^{-2}$. Receiving phase: distilled, deionized water; membrane phase: 0.05 M (HO-heptyl)₂ DC18C6 in phenylhexane in Celgard support. Further details of the experimental procedure are available [37].

^b Interaction is too weak for accurate measurement resulting in an inability to predict and usually to measure J values.

Table VII. Predicted and observed macrocycle-mediated cation fluxes (J) in single and competitive transport experiments in an HFSLM system^a [38].

M^{n+}	Source phase		$J \times 10^8 (mol \cdot sec^{-1} \cdot m^{-2})$	
	Conc. (M)	Predicted	Observed	
1. $K^+NO_3^-$	0.5	32	25 ± 2	
2. $K^+NO_3^-$	0.5	47.7	47 ± 4	
$Na^+NO_3^-$	0.5	<i>b</i>	0.5 ± 0.2	
3. $Sr^{2+}(NO_3^-)_2$	0.1	5.0	4.9 ± 0.6	
$Ba^{2+}(NO_3^-)_2$	0.1	3.2	2.5 ± 0.8	

^a Membrane phase composition: Celgard microporous polypropylene hollow fiber module impregnated with phenylhexane containing dissolved (HO-heptyl)₂DC18C6. Receiving phase: distilled deionized water.

^b Cation anion interaction and macrocycle-mediated extraction are too small for accurate measurement. Hence J cannot be predicted.

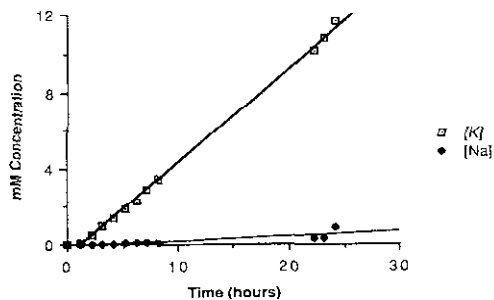


Figure 7. Plot of DC18C6-mediated transport of K^+ and Na^+ as measured by the M^+ concentration in the receiving phase vs. time using a 1MHFSLM system [18]. Source phase: 250 mL solution containing 0.5 M KNO_3 and 0.5 M $NaNO_3$. Membrane phase: 0.1 M DC18C6 in 30 mL octanal. Receiving phase: 250 mL water.

In Figure 7, a plot of the concentrations of K^+ and Na^+ in the receiving phase over a 24-hour period is given for a typical competitive cation experiment [18]. The expected high selectivity of DC18C6 for K^+ over Na^+ is seen. This membrane system has significant advantages that could lead to practical applications.

3. Solid Phase Extraction

3.1. GENERAL

It occurred to us that binding ion-selective macrocycles to solid supports would have several advantages in designing separations systems. First, the chemical bond formed would be permanent and the system could be used indefinitely to perform separations, recoveries, and determinations without measurable loss of the macrocycle. Second, the affinities of the bound macrocycle for ions should be similar to those for the unbound macrocycle in aqueous systems making predictions of ion separations possible. Third, the operating system should be capable of concentrating ions by large amounts since large volumes of feed solution could be passed through the system and the bound ions eluted with a small volume of solution. Fourth, the knowledge and experience of several decades in the design and synthesis of ion-selective macrocycles could be applied to the preparation of hosts capable of pre-determined selective behavior toward specific ion(s) of interest. Fifth, the initial expense associated with the synthesis of the desired macrocycle could be amortized over time because the separation system can be used multiple times and the macrocycle is not lost to the environment. Finally, the SPE procedure would not add new pollutants to the system and the purified species eluted from the separation device would be available for resale. These capabilities of the SPE systems cause them, generally, to be superior to the LM systems in practical chemical separations.

Significant funding to BYU from the State of Utah Centers of Excellence Program (COEP) from 1987 to 1992 provided the means to initiate a program to develop, test, and

commercialize SPE systems. A major purpose of the COEP program was to achieve commercialization of the supported project. This goal was accomplished by the organization of IBC Advanced Technologies, Inc. (IBC). IBC has developed a large number of proprietary SPE materials that are used worldwide in commercial and analytical separations. Descriptions are available of the separations procedure [39-43], and its application to challenging analytical [44] and industrial [45-52] problems. The approach to these problems is based on concepts embodied in molecular recognition. Host molecules are designed and synthesized that are capable of a high degree of recognition for specific guest ions, even when these guests are present at low concentrations and in difficult matrices, such as highly basic, highly acidic, or concentrated solute solutions. The host molecules are attached by chemical bonds through a connector to a solid support, such as silica gel. This is illustrated in Figure 8 for a crown molecule attached to silica gel through a connector. The system of host molecule, connector, and support is termed

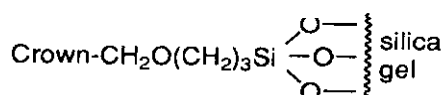


Figure 8. Attachment of macrocycle to silica gel through a connector.

AnaLig™ when used for analytical applications and SuperLig® when used for industrial applications. The AnaLig™ and SuperLig® materials may be used in several configurations such as a packed bed format and incorporated into an Empore™ membrane (3M, St. Paul, MN). MRT is used to describe the process of designing ligands having predetermined ion selectivities, attaching these to supports, and using the resulting AnaLig™ or SuperLig® materials to accomplish desired chemical separations.

Over the past two decades there has been increasing need to separate and recover elements from dilute solutions and difficult matrices. This need has been driven by increasingly more stringent environmental requirements and greater demand for products of increased purity necessitating the removal of contaminants. Determination of trace amounts of the elements involved has become increasingly challenging as the levels have become smaller and the matrices more complex. Use of MRT principles has enabled IBC to accomplish a number of difficult separations. Several of these in the analytical, environmental, metallurgical, precious metal, and nuclear waste areas will now be described. Further detail is given in the cited references.

3.1.1 Analytical

Separation of a specific ion present in trace amounts from a matrix of other ions, often present in high concentrations, is difficult. This difficulty is further enhanced if the additional requirements of speed, efficiency, and high yield are added. Conventional separation techniques are not effective in such cases. An example of such a separation

involving Pb^{2+} from simulated sea water is given in Table VIII [44]. It is seen that Pb^{2+} is recovered quantitatively at the low ppb/high ppt range from a complex and concentrated matrix containing several ions that might be expected to interfere with the separation, but do not.

An important commercial product involving MRT is a disk consisting of AnaLig™ 620 embedded in an Empore™ membrane that selectively removes $^{90}\text{Sr}^{2+}$ from nuclear waste solutions for subsequent analysis. This innovative device received a 1996 R&D 100 Award [54] for the development of a product of high technological significance. It markedly reduces the preparation time and analysis time for $^{90}\text{Sr}^{2+}$ determination. A similar product for Ra^{2+} is also being marketed.

Table VIII. Recovery of Pb^{2+} from simulated seawater^a using AnaLig Pb-02 in the column mode [44].

Pb spike (ppb)	Pb concentration (ppb ± range)	Number of Samples	Pb recovery	
			ppb ± SD ^b	% ± SD ^b
0	0.9 ± 0.2	2	0.85 ± 0.1	94 ± 11
1	1.9 ± 0.2	1	1.7	90
5	5.9 ± 0.3	2	5.8 ± 0.06	98.5 ± 1.1

^aNaCl, 0.459 M; MgSO₄, 0.029 M; MgCl₂, 0.023 M; CaCl₂, 0.010 M; KCl, 0.010 M; NaBr, 8.1 × 10⁻⁴ M; SrCl₂, 1.5 × 10⁻⁴ M; Pb(NO₃)₂, 2.4 × 10⁻⁶ M; Hg (NO₃)₂, 1.5 × 10⁻¹⁰ M.

Values taken from ref. [53].

^bStandard deviation.

3.1.2. Environmental

A major concern in the U.S.A. is environmental contamination. This problem can have many causes including natural events, mining activities, ore processing and refining, industrial processes, and municipal wastes. The offending material often consists of metal ions present in small but potentially hazardous amounts. MRT has great promise for dealing with these problems due to the high selectivity possible even in complex matrices, the ability to process large solution volumes rapidly, the ability to recover the elements in pure form for potential recycling, and the ability to carry out the operation rapidly.

IBC recently tested its MRT process by an onsite separation of the major trace components of Berkeley Pit in Butte, Montana. Berkeley Pit is a large Superfund site resulting from underground and open pit mining operations over the past century[55]. These operations ended in the 1970s. When the pumps were shut down, the open pit began to fill from drainage of the extensive mining operations. The Pit now contains an estimated 100 billion liters of mine waste in a reservoir about 2 km in diameter and 245 meters deep. In tests on site the SuperLig® process was able to perform selective separations, recovery, and purification of trace metals present. The results are summarized

in Table IX [49]. It is seen that each element present was recovered at the >99% level and in highly purified form.

3.1.3. Metallurgical

Mining, ore processing, and preparation of elements of known purity requires varied and complicated separations. These separations usually involve numerous steps, have large space requirements, require large solvent or ion exchange inventories, frequently involve exchange of one impurity for another, and become less effective as contaminants become more dilute. Interest in MRT has stemmed from its promise to overcome these shortcomings of conventional technologies by replacing them with a simpler, faster, and more cost-effective process that has much smaller space requirements.

Table IX. Separation and purification of Berkeley Pit metal constituents [49].

Metal	Feed concentration (mg L ⁻¹)	Treated effluent concentration ^a (mg L ⁻¹)	Recovery (%)	Eluant Purity (%)
Cu	180	<0.02	>99	96-98
Fe	994	<0.1	>99	99.5
Al	270	<1	>99 ^b	97-98
Sn	554	<0.05	>99	99-99.5
Mn	194	<1	>99	75-80 ^b
Cd	2	<0.02	NA ^c	NA ^c
As	0.3	<0.1	NA ^c	NA ^c

^aAll below detection by analytical methods used

^bSome Al slipped past the Al system but was recovered with the Mn. Total Al recovery was >99%.

^cNot analyzed

An example is the control of the bismuth level of copper solutions during refining operations. Bismuth is found as a trace constituent in many copper ore deposits. It concentrates during the refining process and, when certain levels are reached, the quality of the copper product is not acceptable. Maintaining this quality is particularly important today as the demand for high purity metals has increased in the semi-conductor and other fields. Removal of bismuth from aqueous copper solutions by conventional procedures has been difficult. However, MRT procedures have been effective in maintaining acceptable bismuth levels on a continuous basis [50]. Table X gives representative data for bismuth removal from a simulated copper tankhouse solution. It is seen that the bismuth is effectively removed in the presence of a high concentration of copper.

Table X. Removal of bismuth impurity from a copper solution in a copper refinery tankhouse [50].

Stream	Concentration (mg L ⁻¹ or ppm)	
	Bi	Cu
Feed ^a	0.28 x 10 ³	2.96 x 10 ⁴
Barren feed after passing	<i>b</i>	2.91 x 10 ⁴
0.1 M H ₂ SO ₄ wash	<i>b</i>	1.48 x 10 ⁴
Elution	5.65 x 10 ³	<i>b</i>

^aSolutions are in a H₂SO₄ matrix.

^bBelow analytical detection limits.

3.1.4. Precious Metals

For jewelry, catalysis, and other uses, it is necessary to purify palladium, rhodium and other precious metals to 99.995% or better [47,51]. Attainment of this degree of purity poses challenges for the precious metals industry. MRT offers the possibilities of selective recovery of a target precious metal from streams and carrying out the operation rapidly with much smaller space requirements than those of competing technologies. MRT is used to separate palladium from precious metal streams on a commercial scale [51]. An example of the degree of separation possible in the case of palladium is shown in Table XI [52]. It is seen that Pd can be separated in high purity from a large number of competing elements including the chemically similar Pt and Rh.

Table XI. Separation of Pd using SuperLig® 2 from a dilute feed containing Pd, Pt, Rh, and base metals^a [52].

Sample description	Volume (column Volumes)	Concentration (mg L ⁻¹) ^b		
		Pd	Pt	Rh
Original feed	26	610	2,840	345
Feed and wash	30	<1	2,470	295
Elution ^{c,d}	2	7,200	2	<1
Elution ^e tail	2	710	1	<1

^aEluant: 2 M NH₃, 1 M HCl.

^bICP analyzed. [Cl⁻] in feed = 6 M.

^cThe following elements were also analyzed to be <1 mg L⁻¹: Na, K, Ca, Mg, Fe, Cu, Zn, Ni, Co, Mn, Ir, Ru, Cd, Pb, As, Se, Bi, Sb, and Sn.

^dPd(NH₃)₂Cl₂ salt produced by adding HCl to the concentrate yielded a 99.99% pure Pd salt with Pt and Si as the main impurities.

3.1.5. Nuclear Wastes

There is a compelling need for the separation of the components of nuclear waste from storage solutions dating back 50 years or more and from solutions produced by current operation of nuclear reactors for energy generation. Requirements for the separations include resistance to radiation, selective removal often from complex and concentrated matrices, significant reduction in the volume of the solution being treated, and ease of recovery of the target element(s). Present technologies are challenged by these requirements.

One example of the use of MRT in this field was the separation of $^{90}\text{Sr}^{2+}$, discussed earlier. This separation can be carried out on a large scale as shown in Table XII [50].

Table XII. Rapid removal of low-level strontium from Hanford mimic matrix^a using 0.2g of SuperLig® in an Empore disk [50].

Sample description	Sr concentration (mgL ⁻¹ or ppm)
Original solution	100
10 L of feed after column treatment ^b	<1
0-2 mL of 0.03 mol L ⁻¹ Na ₄ EDTA eluent ^b	5 x 10 ⁵
2-4 mL of 0.03 mol L ⁻¹ Na ₄ EDTA eluent ^b	200

^aMatrix with molar concentrations: NaOH, 3.4; NaNO₃, 0.258; NaF, 0.089; NaNO₂, 0.43; Na₂CO₃, 0.23; Na₂HPO₄ · 7 H₂O, 0.025; Na₂SO₄, 0.15; Al(NO₃)₃ · 9 H₂O, 0.43; KNO₃, 0.12; RbNO₃, 0.00005.

^bFlow rate: 40 mL min⁻¹. EDTA = ethylenediaminetetraacetic acid.

The $^{90}\text{Sr}^{2+}$ is readily recovered in a concentrated form by proper elution. The process is continuous since the flow can be directed to a second column while the first is being eluted and prepared for re-use. IBC has SuperLig® materials available for use with many of the components of nuclear waste including strontium, radium, cesium, technetium, and americium.

4.0 Summary

During the past twenty-five years, our effort at BYU has been directed at learning the principles governing a wide variety of selective ion-macrocycle interactions. We have used this knowledge in the design of membrane and solid phase extraction systems capable of highly selective ion separations. Each of these systems has advantages and disadvantages. The solid phase extraction system has the greatest promise for commercial applications. IBC, a spin-off company from our BYU research program, has commercialized SPE in analytical, environmental, metallurgical, precious metal, and

nuclear waste areas. In each of these areas, there is a need for highly selective reagents capable of rapid removal of ions from large volumes of solution, often in the presence of complex matrices that may consist of strong acid, strong base, concentrated salt solutions, or elements having properties similar to those of the target element.

Acknowledgment

Appreciation is expressed to the National Science Foundation, Department of Energy, and Utah Centers of Excellence Program for financial support of our cation-macrocycle and separations investigations over the past twenty-five years. The essential role played by collaborators at BYU and IBC in the work described is acknowledged.

References

1. J.S. Bradshaw and R.M. Izatt: *Acc. Chem. Res.*, in press.
2. J.S. Bradshaw: *J. Incl. Phenom.*, in press.
3. R.M. Izatt, J.H. Rytting, D.P. Nelson, B.L. Haymore, and J.J. Christensen: *Science* **164**, 443 (1969).
4. R.M. Izatt, D.P. Nelson, J.H. Rytting, B.L. Haymore, and J.J. Christensen: *J. Am. Chem. Soc.* **93**, 1619 (1971).
5. R.M. Izatt, R.E. Terry, D.P. Nelson, Y. Chan, D.J. Eatough, J.S. Bradshaw, L.D. Hansen, and J.J. Christensen: *J. Am. Chem. Soc.* **98**, 7626 (1976).
6. R.M. Izatt, R.E. Terry, L.D. Hansen, A.G. Avondet, J.S. Bradshaw, N.K. Dalley, T.E. Jensen, J.J. Christensen, and B.L. Haymore: *Inorg. Chim. Acta* **30**, 1 (1978).
7. H.K. Frensdorff: *J. Am. Chem. Soc.* **93**, 600 (1971).
8. J.-M. Lehn and J.P. Sauvage: *J. Am. Chem. Soc.* **97**, 6700 (1975).
9. D.H. Busch: *Rec. Chem. Progr.* **25**, 107 (1964).
10. J.J. Christensen, D.J. Eatough, and R.M. Izatt: *Chem. Rev.* **74**, 351 (1974).
11. C.J. Pedersen: *J. Am. Chem. Soc.* **89**, 2495 (1967).
12. C.J. Pedersen: *J. Am. Chem. Soc.* **89**, 7017 (1967).
13. C.J. Pedersen: *J. Incl. Phenom.* **6**, 337 (1988).
14. J.-M. Lehn: *J. Incl. Phenom.* **6**, 351 (1988).
15. D.J. Cram: *J. Incl. Phenom.* **6**, 397 (1988).
16. R.M. Izatt, J.D. Lamb, R.L. Bruening: *Sep. Sci. Tech.* **23**, 1645 (1988).
17. R.M. Izatt, J.S. Bradshaw, J.D. Lamb, and R.L. Bruening: in T. Araki and H. Tsukube (eds.), *Liquid Membranes: Chemical Applications*; CRC Press: Boca Raton, FL, Chapter 7.1 (1990), p 123.
18. J.D. Lamb, R.L. Bruening, D.A. Linsley, C. Smith, and R.M. Izatt: *Sep. Sci. Tech.* **25**, 1407 (1990).
19. J.D. Lamb, R.L. Bruening, R.M. Izatt, Y. Hirashima, P.-K. Tse, and J.J. Christensen: *J. Membrane Sci.* **37**, 13 (1988).
20. R.M. Izatt, G.A. Clark, J.S. Bradshaw, J.D. Lamb, and J.J. Christensen: *Sep. Purif. Meth.* **15**, 21 (1986).
21. J.J. Christensen, J.D. Lamb, S.R. Izatt, S.E. Starr, G.C. Weed, M.S. Astin, B.D. Stitt, and R.M. Izatt: *J. Am. Chem. Soc.* **100**, 3219 (1978).
22. J.D. Lamb, J.J. Christensen, S.R. Izatt, K. Bedke, M.S. Astin, and R.M. Izatt: *J. Am. Chem. Soc.* **102**, 3399 (1980).
23. M. Kirch, and J.M. Lehn: *Angew. Chem. Internat. Edit.* **14**, 555 (1975).
24. J.D. Lamb, J.J. Christensen, J.L. Oscarson, B.L. Nielsen, B.W. Asay, and R.M. Izatt: *J. Am. Chem. Soc.* **102**, 6820 (1980).
25. J.D. Lamb, R.M. Izatt, P.A. Robertson, and J.J. Christensen: *J. Am. Chem. Soc.* **102**, 2452 (1980).
26. R.M. Izatt, J.D. Lamb, R.T. Hawkins, P.R. Brown, S.R. Izatt, and J.J. Christensen: *J. Am. Chem. Soc.* **105**, 1782 (1983).
27. S.R. Izatt, R.T. Hawkins, J.J. Christensen, and R.M. Izatt: *J. Am. Chem. Soc.* **107**, 63 (1985).

28. J.D. Lamb, P.R. Brown, J.J. Christensen, J.S. Bradshaw, D.G. Garrick, and R.M. Izatt: *J. Membrane Sci.* **13**, 89 (1983).
29. R.M. Izatt, R.M. Haws, J.D. Lamb, D.V. Dearden, P.R. Brown, D.W. McBride Jr., and J.J. Christensen: *J. Membrane Sci.* **20**, 273 (1984).
30. R.M. Izatt, D.W. McBride Jr., J.J. Christensen, J.S. Bradshaw, and G.A. Clark: *J. Membrane Sci.* **22**, 31 (1985).
31. R.M. Izatt, G.C. LindH, R.L. Bruening, P. Huszthy, C., W. McDaniel, J.S. Bradshaw, and J.J. Christensen: *Anal. Chem.* **60**, 1694 (1988).
32. R.M. Izatt, M.P. Biehl, J.D. Lamb, and J.J. Christensen: *Sep. Sci. Tech.* **17**, 1351 (1982).
33. R.M. Izatt, J.S. Bradshaw, S.A. Niclsen, J.D. Lamb, J.J. Christensen, D. Sen: *Chem. Rev.* **85**, 271 (1985).
34. J.J. Christensen, S.P. Christensen, M.P. Biehl, S.A. Lowe, J.D. Lamb, and R.M. Izatt: *Sep. Sci. Tech.* **18**, 363 (1983).
35. R.M. Izatt, R.L. Bruening, W. Geng, M.H. Cho, and J.J. Christensen: *Anal. Chem.* **59**, 2405 (1987).
36. R.M. Izatt, R.L. Bruening, M.H. Cho, W. Geng, J.D. Lamb, and J.J. Christensen: *J. Membrane Sci.* **33**, 169 (1987).
37. R.M. Izatt, R.L. Bruening, M.L. Bruening, G.C. LindH, and J.J. Christensen: *Anal. Chem.* **61**, 1140 (1989).
38. R.M. Izatt, D.K. Roper, R.L. Bruening, and J.D. Lamb: *J. Membrane Sci.* **45**, 73 (1989).
39. J.S. Bradshaw, R.L. Bruening, K.E. Krakowiak, B.J. Tarbet, M.L. Bruening, and R.M. Izatt, (the late) J.J. Christensen: *J. Chem. Soc., Chem. Commun.*, 812 (1988).
40. J.S. Bradshaw, R.M. Izatt, J.J. Christensen, K.E. Krakowiak, B.J. Tarbet, R.L. Bruening, S. Lifson: *J. Incl. Phenom.* **7**, 27 (1989).
41. R.M. Izatt, J.S. Bradshaw, R.L. Bruening, B.J. Tarbet, and M.L. Bruening: *Pure Appl. Chem.* **67**, 1069 (1995).
42. M.L. Bruening, D.M. Mitchell, R.M. Izatt, and R.L. Bruening: *Sep. Sci. Tech.* **26**, 761 (1991).
43. R.M. Izatt, J.S. Bradshaw, and R.L. Bruening: *Pure Appl. Chem.* **68**, 1237 (1996).
44. R.M. Izatt, J.S. Bradshaw, R.L. Bruening, and M.L. Bruening: *Am. Lab.* **26**, 28c (1994).
45. R.M. Izatt, J.S. Bradshaw, R.L. Bruening, B.J. Tarbet, and K.E. Krakowiak: in V.I. Lakshmanan, et al. (eds.), *Emerging Separation Technologies for Metals and Fuels*, TMS: Warrendale, PA, (1993) p. 67.
46. N.E. Izatt, R.L. Bruening, L. Anthian, L.D. Griffin, B.J. Tarbet, R.M. Izatt, and J.S. Bradshaw: in H.Y. Sohn, (ed.), *Proceedings: Metallurgical Processes for Early 21st Century*, Warrendale, PA, TMS, (1994) p. 1001.
47. R.L. Bruening, J.B. Dale, N.E. Izatt, and W. Young: in *Hidden Wealth*, South African Institute of Mining and Metallurgy, Johannesburg, (1996) p. 143.
48. R.L. Bruening, J.B. Dale, N.E. Izatt, and W. Young: in *Hidden Wealth*, South African Institute of Mining and Metallurgy, Johannesburg, (1996) p. 45.
49. R.L. Bruening, N.E. Izatt, W. Young, and P. Soto: in M.A. Sánchez, F. Vergara, and S.H. Castro (eds.), *Clean Technology for the Mining Industry*, Univ. Of Concepción, Concepción, Chile (1996).
50. R.M. Izatt, J.S. Bradshaw, R.L. Bruening, B.J. Tarbet, and M.L. Bruening, in D.N. Reinhoudt, (ed.), *Comprehensive Supramolecular Chemistry, Vol. 10, Supramolecular Technology*, Elsevier, Tarrytown, NY, (1996) p. 1.
51. C. Wright and R.L. Bruening: *Proceedings of a Seminar of the International Precious Metals Institute*, Scottsdale, AZ, 95 (1989).
52. R.L. Bruening, J.B. Dale, R.M. Izatt, and S.R. Izatt: Presented at the Spring 1995 National AIChE Meeting, March 19-23, 1995.
53. *CRC Handbook of Chemistry and Physics*, 73rd Ed., D.R. Lide (ed.), CRC Press, Boca Raton, FL, 1992-1993, p. 14.
54. *R&D Magazine*, **38**, (10) 21 (1996).
55. D. Baum and M.L. Knox: *Smithsonian*, **23**, 46 (1992).